

# NUCLEON EDM FROM ATOMIC SYSTEMS AND CONSTRAINTS ON SUPERSYMMETRY PARAMETERS

Sachiko Oshima,<sup>1</sup> Takeshi Nihei,<sup>2,\*</sup> and Takehisa Fujita<sup>2,†</sup>

<sup>1</sup>*Department of Physics, Faculty of Science, Tokyo Institute of Technology, Tokyo, Japan*

<sup>2</sup>*Department of Physics, Faculty of Science and Technology, Nihon University, Tokyo, Japan*

(Dated: February 5, 2018)

The nucleon EDM is shown to be directly related to the EDM of atomic systems. From the observed EDM values of the atomic Hg system, the neutron EDM can be extracted, which gives a very stringent constraint on the supersymmetry parameters. It is also shown that the measurement of Nitrogen and Thallium atomic systems should provide important information on the flavor dependence of the quark EDM. We perform numerical analyses on the EDM of neutron, proton and electron in the minimal supersymmetric standard model with CP-violating phases. We demonstrate that the new limit on the neutron EDM extracted from atomic systems excludes a wide parameter region of supersymmetry breaking masses above 1 TeV, while the old limit excludes only a small mass region below 1 TeV.

PACS numbers: 12.60.Jv, 13.40.Em, 11.30.Er, 14.20.Dh, 21.10.Ky, 24.80.+y

## I. INTRODUCTION

In field theory, it is important to understand the property of the symmetry of the Lagrangian density. In the standard model, the time reversal invariance is normally kept, but due to the phase of Kobayashi-Maskawa mixing matrix, there is the T-violation term present in the Lagrangian density. The phase shows up as the CP violation effects on the  $K^0 - \bar{K}^0$  mixing in the kaon decay processes [1, 2]. Since the CP violation of the Kaon decay experiment determines the Kobayashi-Maskawa phase, it should be interesting to see what should be further physical observables which are predicted from the CP violation phenomena or T-violating observables.

Recent experiments on the CP violation of the  $B^0 - \bar{B}^0$  mixing in the B-meson decay processes suggest that the phase of Kobayashi-Maskawa mixing matrix may not be able to describe the observed mixing angle from the  $B^0 - \bar{B}^0$  mixing. This suggests that there may be some other terms present in the Lagrangian density, which violates the T-invariance.

The direct measurement of the T-violation effects can be examined if one can measure the electric dipole moments (EDM) of the isolated system. The finite number of the neutron EDM should exhibit most clearly the direct evidence of the T-violation effects in the Lagrangian density. Until now, the upper limit of the neutron EDM  $d_n$  from the direct measurements is around [3, 4, 5]

$$d_n \simeq (1.9 \pm 5.4) \times 10^{-26} \text{ e} \cdot \text{cm} \quad (1.1a)$$

$$d_n \simeq (2.6 \pm 4.0 \pm 1.6) \times 10^{-26} \text{ e} \cdot \text{cm}. \quad (1.1b)$$

This EDM is still not finite, but gives a strong constraint on the supersymmetry model parameters.

There are also EDM measurements of atomic systems such as  $^{129}\text{Xe}$  [6, 7] and  $^{199}\text{Hg}$  [8, 9]. However, it is not very easy to extract the individual particles EDM from the atomic EDM measurements since there is the Schiff theorem [10]. The Schiff theorem states that the EDM of the individual particles cannot be measured if the constituents are interacting with nonrelativistic static Coulomb force. The EDM of the individual particles should show up when they are interacting with relativistic kinematics [11, 12, 13] or with strong interactions [14]. The EDM due to the former case is found in the heavy atomic system while the EDM of the latter case arises from the finite nuclear size effects.

Recent careful studies clarify [15] that the EDM arising from the nuclear finite size effects is directly related to the neutron EDM  $d_n$  as

$$d_{\text{Xe}} \simeq 1.6d_n \quad (1.2a)$$

$$d_{\text{Hg}} \simeq -2.8d_n \quad (1.2b)$$

where  $d_{\text{Xe}}$  and  $d_{\text{Hg}}$  denote the EDMs of Xe and Hg atomic systems. In particular, the EDM of  $^{199}\text{Hg}$  atomic system is observed with high accuracy and from the observed value of  $d_{\text{Hg}}$ , we can deduce the neutron EDM as

$$d_n \simeq (0.37 \pm 0.17 \pm 0.14) \times 10^{-28} \text{ e} \cdot \text{cm}. \quad (1.3)$$

This number is three orders of magnitude smaller than the direct measurement of neutron EDM in eq.(1.1). Therefore, it should be worthwhile to examine how this number of the neutron EDM can give constraints on the supersymmetry model parameters.

Supersymmetry (SUSY) is one of the most promising candidates for new physics beyond the standard model [16]. In particular, supersymmetric models contain new CP-violating phases [17] in addition to the phase of the Cabbibo-Kobayashi-Maskawa mixing matrix, and the effect of these phases may explain the discrepancy between the experimental result and the standard model

\*Electronic address: nihei@phys.cst.nihon-u.ac.jp

†Electronic address: ffujita@phys.cst.nihon-u.ac.jp

prediction for CP-asymmetry in the B-meson decays. In general, the new CP-violating phases in supersymmetric models induce a non-vanishing EDM for quarks and leptons. In fact, they give a large contribution to the EDMs at the one-loop level. On the other hand, it is known that the standard model contributions to the EDMs cancel out up to the two-loop level, and the leading three-loop contribution is much smaller than the current experimental upper bound. This implies that a large EDM is not only a signal of CP-violation but also an indirect evidence of SUSY.

In the present work, we calculate the EDM of neutron, proton and electron in the minimal supersymmetric standard model (MSSM) with CP-violating phases. We shall show that the neutron EDM limit in eq.(1.3) gives a very severe constraint on the parameters in the supersymmetric model. For a sizable value of the CP-violating phases, the magnitude of soft breaking mass parameters typically has to be larger than several TeV to satisfy the EDM constraint.

Further, we show, for the first time, that the proton EDM can be extracted from the Nitrogen and Thallium atomic EDM. This is simply because, for the  $^{15}\text{N}$  case, it has the ground state with spin  $1/2$ , and the state is described by the proton hole state as  $|\pi(1p_{\frac{1}{2}})^{-1} : \frac{1}{2}^{-}\rangle$  to a good accuracy. Also, for the  $^{205}\text{Tl}$  case, since it is a single proton hole state, it can be expressed as  $|\pi(3s_{\frac{1}{2}})^{-1} : \frac{1}{2}^{+}\rangle$  to a good approximation even though the neutrons are not in the magic but in the two hole state.

From the experimental constraint, the nucleus should have the spin  $1/2$  such that the quadrupole field should not have any effects on the EDM measurements. In this respect,  $^{15}\text{N}$  and  $^{205}\text{Tl}$  atomic systems must be good cases for measuring the nuclear EDM. The EDM of the Nitrogen atomic system  $d_{^{15}\text{N}}$  and the  $^{205}\text{Tl}$  atomic system  $d_{\text{Tl}}$  are related to the proton EDM  $d_p$ , and the calculated numbers become

$$d_{^{15}\text{N}} \simeq -0.16d_p \quad (1.4a)$$

$$d_{\text{Tl}} \simeq 4.8d_p. \quad (1.4b)$$

Recently, Regan et.al have measured the atomic EDM of  $^{205}\text{Tl}$  by the atomic beam magnetic resonance method [18]. From the measurement of the atomic EDM of  $^{205}\text{Tl}$ , we can extract the proton EDM  $d_p$

$$d_p \simeq -(0.83 \pm 0.90) \times 10^{-25} \text{ e} \cdot \text{cm} \quad (1.5)$$

which is quite a severe constraint on the proton EDM  $d_p$ . Here, we have not included the electron EDM contribution to the atomic EDM of  $^{205}\text{Tl}$ , and the electron EDM contribution will be discussed in a qualitative manner in section 4.

On the other hand, the EDM for the Nitrogen case is smaller than the ones in heavier nuclei, but we believe that the Nitrogen EDM should be also measured in future.

This paper is organized as follows. In the next section, we briefly discuss the new mechanism to obtain the EDM of the individual particles in nucleus, like neutron EDM or proton EDM from atomic systems. Then, in section 3, we evaluate the EDM of neutron, proton and electron in the minimal supersymmetric standard model with CP-violating phases, and find various constraints on the supersymmetric parameters from the observed neutron EDM value. In section 4, we present a qualitative discussion on the contributions of the electron and the proton EDMs to the atomic EDM value. Section 5 summarizes what we clarify the nuclear EDM and the related parameters which appear in the supersymmetry models.

## II. NUCLEON EDM FROM ATOMIC SYSTEMS

The electric dipole moment (EDM) of the isolated system can present a direct evidence of the T-violation interaction if it is finite. Since the measurement is carried out for the total atomic system, the EDM of the individual particles (electron EDM or nucleon EDM) should be extracted from the atomic EDM measurement. However, this extraction is a nontrivial task since there is the Schiff theorem. The Schiff theorem states that the EDM of the individual particles cannot be measured if the neutral system is interacting with nonrelativistic electrostatic forces.

The EDM of electron becomes important when the system has a relativistic effect since the Schiff theorem is not applicable to the relativistic case. Indeed for heavier atoms, the relativistic effect becomes important since the relativistic correction is seen as  $(Z\alpha)^2$ . For the electron EDM, there are many calculations in heavy atoms.

If the interactions are due to nuclear forces, then there is no effect from the Schiff theorem. Since the nucleus is always found in atomic system, the nuclear EDM can be seen as the finite size effects in the total atomic system. Recent calculations on the nuclear EDM show that there is an appreciably large effect of the nuclear EDM to the total atomic EDM after the effects due to the Schiff theorem are taken into account. The results obtained in [15] for Xe and Hg atomic EDM are summarized in eqs. (1.2).

Now, we briefly describe the finite size effects of the atomic EDM since the detailed calculation is found in [15]. In particular, the effects due to the Schiff theorem are well treated and explained in [15], and therefore we do not repeat it for this part in this paper.

### A. Hamiltonian of atomic systems

We first write the Hamiltonian of the total atomic and nuclear systems for Nitrogen.

The unperturbed Hamiltonian  $H_0$  of the Nitrogen sys-

tem can be written

$$H_0 = \sum_{i=1}^Z \left[ \frac{\mathbf{p}_i^2}{2m} - \sum_{j=1}^Z \frac{e^2}{|\mathbf{r}_i - \mathbf{R}_j|} \right] + \frac{1}{2} \sum_{i \neq j}^Z \frac{e^2}{|\mathbf{r}_i - \mathbf{r}_j|} \\ + \sum_{i=1}^A \frac{\mathbf{P}_i^2}{2M} + \frac{1}{2} \sum_{i \neq j}^A V_{NN}(|\mathbf{R}_i - \mathbf{R}_j|) + \frac{1}{2} \sum_{i \neq j}^Z \frac{e^2}{|\mathbf{R}_i - \mathbf{R}_j|} \quad (2.1)$$

where  $\mathbf{r}_i$ ,  $\mathbf{p}_i$  denote the coordinate and the momentum of the electron while  $\mathbf{R}_i$ ,  $\mathbf{P}_i$  denote the nuclear variable and momentum, respectively.

On the other hand, the perturbed Hamiltonian coming from the EDM is written as

$$H_{edm} = - \sum_{i=1}^Z \sum_{j=1}^Z \frac{e \mathbf{d}_e^i \cdot (\mathbf{r}_i - \mathbf{R}_j)}{|\mathbf{r}_i - \mathbf{R}_j|^3} + \sum_{i=1}^Z \sum_{j \neq i}^Z \frac{e \mathbf{d}_e^i \cdot (\mathbf{r}_i - \mathbf{r}_j)}{|\mathbf{r}_i - \mathbf{r}_j|^3} \\ - \sum_{i=1}^Z \sum_{j=1}^A \frac{e \mathbf{d}_N^j \cdot (\mathbf{r}_i - \mathbf{R}_j)}{|\mathbf{r}_i - \mathbf{R}_j|^3} - \sum_{i=1}^A \sum_{j \neq i}^Z \frac{e \mathbf{d}_N^i \cdot (\mathbf{R}_i - \mathbf{R}_j)}{|\mathbf{R}_i - \mathbf{R}_j|^3} \\ - \sum_{i=1}^Z \mathbf{d}_e^i \cdot \mathbf{E}_{ext} - \sum_{i=1}^A \mathbf{d}_N^i \cdot \mathbf{E}_{ext} + e \sum_{i=1}^Z (\mathbf{r}_i - \mathbf{R}_i) \cdot \mathbf{E}_{ext} \quad (2.2)$$

where the summation over  $Z$  in nucleus means that it should be taken over protons. The EDM of the nucleon can be expressed in terms of the nucleon isospin as

$$\mathbf{d}_N^i = \frac{1}{2} [(1 + \tau_i^z) d_p \boldsymbol{\sigma}^i + (1 - \tau_i^z) d_n \boldsymbol{\sigma}^i]. \quad (2.3)$$

### B. Nuclear EDM from nuclear excitation

Here, we evaluate the finite size effects on the second order EDM energy in the nucleus. The perturbed EDM Hamiltonian for nuclear parts  $H_{edm}^{(n)}$  can be written as

$$H_{edm}^{(n)} = - \sum_{i=1}^A \sum_{j \neq i}^Z e \mathbf{d}_N^i \cdot \frac{(\mathbf{R}_i - \mathbf{R}_j)}{|\mathbf{R}_i - \mathbf{R}_j|^3} - \frac{e}{2} \sum_{i=1}^A (1 + \tau_i^z) \mathbf{R}_i \cdot \mathbf{E}_{ext}. \quad (2.4)$$

Now, we consider the second order EDM energy due to the intermediate nuclear excitations, keeping the atomic state in the ground state. This process arises from the finite nuclear size effects in the EDM Hamiltonian. The second order EDM energy can be written as

$$\Delta E_{fs}^{(2)} = - \sum_n \frac{e^2}{E_n - E_0} \langle \Psi_N | \sum_{i=1}^A \tau_i^z \mathbf{R}_i \cdot \mathbf{E}_{ext} | n \rangle \\ \times \langle n | \sum_{i \neq j}^A \frac{1}{4} [(1 + \tau_i^z) d_p \boldsymbol{\sigma}^i + (1 - \tau_i^z) d_n \boldsymbol{\sigma}^i]$$

$$\cdot \frac{(1 + \tau_j^z) (\mathbf{R}_i - \mathbf{R}_j)}{|\mathbf{R}_i - \mathbf{R}_j|^3} | \Psi_N \rangle \quad (2.5)$$

where  $E_0$  and  $E_n$  denote the ground state energy and the excitation energy of the nuclear states, respectively. The electron states are kept in the ground state throughout the calculation, and therefore it is not written here. Also, it should be noted that we made use of the relation  $\sum_{i=1}^A \mathbf{R}_i = 0$  since we set the center mass coordinate to the nuclear center.

### C. Nitrogen atomic system

Now, we calculate the  $^{15}\text{N}$  case in which we assume a simple single particle shell model state  $|\pi(1p_{\frac{1}{2}})^{-1}\rangle$ . This should be rather a good description for  $^{15}\text{N}$ . Further, the atomic states stay in the ground state, and therefore the electron wave functions are not written here. Thus, we write the nuclear wave function as

$$|\Psi_N\rangle = |\pi(1p_{\frac{1}{2}})^{-1} : \frac{1}{2}^{-}\rangle. \quad (2.6)$$

In this case, the intermediate states  $|n\rangle$  that contribute to the second order EDM energy [eq.(2.6)] for  $\pi(1p_{\frac{1}{2}})$  are restricted to

$$|n\rangle = |\pi(1s_{\frac{1}{2}})^{-1} : \frac{1}{2}^{+}\rangle, \quad |\pi(1p_{\frac{1}{2}})^{-2}, \pi(2s_{\frac{1}{2}}) : \frac{1}{2}^{+}\rangle. \quad (2.7)$$

With eqs.(2.5-7), we carry out numerical calculations of the second order EDM energy  $\Delta E_{fs}^{(2)}$  and obtain the relation between the Nitrogen EDM  $d_{^{15}\text{N}}$  and the proton EDM  $d_p$  as

$$d_{^{15}\text{N}} \simeq -0.16 d_p. \quad (1.4a)$$

Even though the factor in front of  $d_p$  is not very large number, we believe that the EDM of Nitrogen can be well measured experimentally in future.

### D. Thallium atomic system

Now, we calculate the  $^{205}\text{Tl}$  case in which we assume a simple single particle shell model state  $|\pi(3s_{\frac{1}{2}})^{-1}\rangle$ . This should be reasonable for the  $^{205}\text{Tl}$  case. Therefore, the nuclear wave function for  $^{205}\text{Tl}$  can be written as

$$|\Psi_N\rangle = |\pi(3s_{\frac{1}{2}})^{-1} : \frac{1}{2}^{+}\rangle. \quad (2.8)$$

In this case, the intermediate states  $|n\rangle$  that contribute to the second order EDM energy [eq.(2.6)] for  $|\pi(3s_{\frac{1}{2}})^{-1}\rangle$  are restricted to

$$|n\rangle = |\pi(2p_{\frac{1}{2}})^{-1} : \frac{1}{2}^{-}\rangle, \quad |\pi(3s_{\frac{1}{2}})^{-2}, \pi(3p_{\frac{1}{2}}) : \frac{1}{2}^{-}\rangle. \quad (2.9)$$

With eqs.(2.8-9), we carry out numerical calculations of the second order EDM energy  $\Delta E_{fs}^{(2)}$  and obtain the relation between the Thallium EDM  $d_{T\ell}$  and the proton EDM  $d_p$  as

$$d_{T\ell} \simeq 4.8d_p. \quad (1.4b)$$

Clearly, the EDM of Thallium is quite large, and therefore there must be a good chance of observing it. Indeed, there is a measurement of TlF compound system, and Cho et al. [19] obtained the EDM of  $d_{T\ell F}$  as

$$d_{T\ell F} \simeq (-1.7 \pm 2.9) \times 10^{-23} \text{ e} \cdot \text{cm}. \quad (2.10)$$

Making use of the relation between Thallium EDM and proton EDM [eq.(1.4b)], we obtain the proton EDM as

$$d_p \simeq (-0.35 \pm 0.60) \times 10^{-23} \text{ e} \cdot \text{cm} \quad (2.11)$$

where we ignored the contribution of EDM from the Fluoride atomic system.

Further, Regan et al. have recently measured the atomic EDM of  $^{205}\text{Tl}$  by the atomic beam magnetic resonance method [18]. They extracted the electron EDM from their measurement, and obtained the constraint of electron EDM  $d_e$ . Here, we estimate the proton EDM from their measurements, and the atomic EDM of  $^{205}\text{Tl}$  is found to be

$$d_{T\ell} \simeq -(0.4 \pm 0.43) \times 10^{-24} \text{ e} \cdot \text{cm}. \quad (2.12)$$

Therefore, we can extract the proton EDM using eq.(1.4b)

$$d_p \simeq -(0.83 \pm 0.90) \times 10^{-25} \text{ e} \cdot \text{cm} \quad (2.13)$$

which gives stronger constraints than eq.(2.11) of Cho et.al almost by two orders of magnitude. This proton value of  $d_p$  is just comparable to the neutron EDM  $d_n$  from the direct measurement.

As mentioned above, the effects due to the electron EDM  $d_e$  in heavy atoms should be large. In fact the contribution of the electron EDM to the Thallium case is evaluated in [20], and they found a very large enhancement factor. In this paper, however, we have not included the electron EDM. Instead, we will discuss the electron EDM contribution to the atomic EDM in a qualitative fashion in section 4.

### III. CONSTRAINTS FROM NEUTRON EDM ON SUPERSYMMETRY MODEL

In this section, we discuss the constraints from the neutron EDM in the MSSM. In the present analysis, we work in a framework of a phenomenological MSSM. The relevant parameters in this model are defined as follows. SUSY breaking mass terms for the squarks and the sleptons contain a common scalar mass parameter  $m_0$  as

$$-m_0^2(|\tilde{q}|^2 + |\tilde{u}|^2 + |\tilde{d}|^2 + |\tilde{\ell}|^2 + |\tilde{e}|^2), \quad (3.1)$$

where  $\tilde{q}$  and  $\tilde{\ell}$  denote the SU(2) doublet fields for the left-handed squarks and sleptons, respectively, while  $\tilde{u}$ ,  $\tilde{d}$  and  $\tilde{e}$  denote the SU(2) singlet fields for the right-handed scalar up-quark, the scalar down-quark and the scalar electron, respectively. Gaugino mass terms for the bino  $\tilde{B}$ , the wino  $\tilde{W}^a$  ( $a = 1, 2, 3$ ) and the gluino  $\tilde{g}^\alpha$  ( $\alpha = 1, \dots, 8$ ) are given by

$$-\frac{1}{2}(M_1\tilde{B}\tilde{B} + M_2\tilde{W}^a\tilde{W}^a + M_3\tilde{g}^\alpha\tilde{g}^\alpha) + \text{h.c.}, \quad (3.2)$$

where  $M_1$ ,  $M_2$  and  $M_3$  denote a mass parameter for  $U(1)_Y$ ,  $SU(2)_L$  and  $SU(3)_C$  gaugino, respectively. We assume the GUT relation for the gaugino masses  $M_1 = \frac{5}{3}\tan^2\theta_W M_2$  and  $M_3 = \frac{\alpha_3}{\alpha_2} M_2$ .

The SUSY conserving part of the Lagrangian can be written by the superpotential

$$W = Y_u\hat{U}^c\hat{H}_2\hat{Q} + Y_d\hat{D}^c\hat{H}_1\hat{Q} + Y_e\hat{E}^c\hat{H}_1\hat{L} + \mu\hat{H}_1\hat{H}_2, \quad (3.3)$$

where  $Y_u$ ,  $Y_d$  and  $Y_e$  are Yukawa couplings for the up-quark, the down-quark and the electron, respectively. The coefficient  $\mu$  is a Higgs mixing mass parameter. The symbols with a hat denote chiral superfields with self-evident notations. In eq.(3.3), we neglect generation mixings, since we discuss generation conserving effects. The scalar trilinear couplings are parameterized by the universal mass parameter  $A$  as

$$A(Y_u\tilde{u}^*H_2\tilde{q} + Y_d\tilde{d}^*H_1\tilde{q} + Y_e\tilde{e}^*H_1\tilde{\ell}). \quad (3.4)$$

Furthermore, the Higgs sector in this model includes the ratio of the vacuum expectation values of the two neutral Higgs fields,  $\tan\beta = \langle H_2 \rangle / \langle H_1 \rangle$ , and a mass parameter  $m_A$  for the pseudoscalar neutral Higgs field.

In summary, the Lagrangian is parameterized by the following parameters

$$\tan\beta, m_A, M_2, m_0, \mu, A. \quad (3.5)$$

Among these,  $M_2$ ,  $\mu$  and  $A$  can have a non-vanishing complex phase. We take a phase convention that  $M_2$  is real and positive. In order to examine the effects of CP-violation, we define two complex phases ( $\theta_\mu, \theta_A$ ) by

$$\mu = |\mu|\exp(i\theta_\mu), \quad A = |A|\exp(i\theta_A). \quad (3.6)$$

The EDMs of quarks and leptons are defined as a coefficient in the electric dipole operator

$$\mathcal{L} = -\frac{i}{2}d_f\bar{f}\sigma_{\mu\nu}\gamma_5 f F^{\mu\nu}. \quad (3.7)$$

The EDM  $d_f$  of the fermion  $f$  ( $= u, d, e$ ) can be obtained by evaluating relevant Feynman diagrams. In the case of the MSSM, three kinds of diagrams contribute at the one-loop level: (i) chargino exchange contribution, (ii) neutralino exchange contribution and (iii) gluino exchange contribution. Note that the gluino contribution

does not exist for the electron EDM  $d_e$ . The expression of  $d_f$  for each fermion can be found in Ref. [21].

To obtain the EDM of the neutron and the proton, we employ the non-relativistic quark model as

$$d_n = \frac{1}{3}(4d_d - d_u), \quad d_p = \frac{1}{3}(4d_u - d_d). \quad (3.8)$$

It should be noted that a quark chromomagnetic dipole operator and a pure gluonic dipole operator may give comparable contributions to the electric dipole operator (3.7) [23]. Inclusion of these operators may cause cancellations to suppress the neutron EDM. However, this kind of cancellations occurs in relatively small portions of the whole parameter space. Therefore, we neglect the effects of these operators for simplicity. Also, we focus on a nuclear finite size effects, and neglect contributions from the chromomagnetic dipole operator for the strange quark [24] in this analysis.

In the following, we present the results of our numerical analysis. In all the figures, we always choose  $\tan\beta = 10$  and  $m_A = 700$  GeV as reference values. For large  $\tan\beta$ , the EDMs are typically enhanced so that the constraint on the mass parameters becomes more stringent. The EDMs are not very sensitive to  $m_A$ , since the Higgs masses are not directly related with the relevant diagrams.

Let us begin with the effect of  $\theta_A$  assuming that  $\mu$  is real and positive. Variations of the EDMs in the  $(M_2, m_0)$  plane are displayed in Fig. 1 for  $\tan\beta = 10$ ,  $m_A = 700$  GeV,  $|\mu| = 500$  GeV,  $|A| = 500$  GeV,  $\theta_\mu = 0$ ,  $\theta_A = \pi/6$ . The result for the neutron EDM is shown in the upper left window. If we assume previous experimental limit  $d_n \lesssim 10^{-25}$  using the neutron itself, only the small mass region  $m_0, M_2 \lesssim 1$  TeV would be excluded. However, with the new limit

$$0.06 \times 10^{-28} \text{e} \cdot \text{cm} < d_n < 0.68 \times 10^{-28} \text{e} \cdot \text{cm} \quad (3.9)$$

derived from eq.(1.3), it is found that the large region below the solid line is excluded by the neutron EDM.

In the upper right window of the same figure, we plot the contours of the proton EDM for the same choice of the parameters. In this case,  $d_p$  is negative in the whole region. As for the magnitude,  $|d_p|$  is of the same order of magnitude as  $d_n$ . This can be seen more clearly in the contour plot of the ratio  $d_p/d_n$  (lower left window). In the region  $M_2 \gg m_0$ ,  $|d_p|$  is smaller than  $d_n$ , while it is nearly equal to  $d_n$  for  $M_2 \lesssim m_0$ .

For comparison, we also plot the contours of  $d_e$  in the lower right window. The current experimental upper bound for the electron EDM is  $|d_e| < 1.6 \times 10^{-27} \text{e} \cdot \text{cm}$  [18]. We can see that the constraint from  $d_n$  is much severer than that from  $d_e$ .

The effect of varying  $\theta_A$  can be seen in the  $(m_0, \theta_A)$  plane in Fig. 2 for  $\tan\beta = 10$ ,  $m_A = 700$  GeV,  $M_2 = 1$  TeV,  $|\mu| = 500$  GeV,  $|A| = 500$  GeV,  $\theta_\mu = 0$ . For  $0 < \theta_A < \pi$ ,  $d_n$  is positive, and only small regions outside the solid lines are allowed by the neutron EDM constraint (3.9). In

particular, for  $0.2\pi \lesssim \theta_A \lesssim 0.8\pi$ , the common sfermion mass  $m_0$  must be larger than 10 TeV to satisfy (3.9) for this choice of the parameters. For  $\pi < \theta_A < 2\pi$ ,  $d_n$  is negative.

Finally, we discuss the effect of  $\theta_\mu$ . The phase dependence of the neutron EDM for fixed  $m_0$  and  $M_2$  is shown in Fig. 3. The relevant supersymmetric parameters for the upper window are chosen as  $\tan\beta = 10$ ,  $m_A = 700$  GeV,  $M_2 = 2$  TeV,  $m_0 = 5$  TeV,  $|\mu| = 500$  GeV,  $|A| = 500$  GeV and  $\theta_A = 0$ , while those for the lower window are the same except  $\theta_\mu = 0$ . The range  $0 < \theta_\mu < \pi$  in the upper window and the range  $\pi < \theta_A < 2\pi$  in the lower window corresponds to  $d_n < 0$ . In the region between the two dashed lines, the EDM constraint (3.9) is satisfied. From the two plots, we see that the CP-violating phases  $\theta_\mu$  and  $\theta_A$  are severely bound to zero even in a multi-TeV region of SUSY breaking mass parameters. Relatively speaking,  $\theta_A$  is less constrained than  $\theta_\mu$ . Therefore, if we take sizable  $\theta_\mu$  rather than  $\theta_A$ , the constraints on  $m_0$  and  $M_2$  become severer than those in figures 1 and 2.

#### IV. DISCUSSIONS ON $d_e$ AND $d_p$

The expected magnitudes of the electron EDM  $d_e$  and the proton EDM  $d_p$  depend on the parameters of the SUSY models. It should be rather difficult to reliably predict the relative magnitude between  $d_e$  and  $d_p$ .

Therefore, the contributions from  $d_e$  and  $d_p$  to the atomic EDM values should be estimated carefully. In this paper, we do not include any contributions of the electron EDM, but instead we will discuss the electron EDM contribution to the atomic EDM in a qualitative fashion.

Below, we evaluate the contributions from  $d_e$  and  $d_p$  to the Nitrogen and Thallium atomic EDMs.

##### A. Electron EDM in atomic system

The electron EDM contributions to the atomic EDM come from the relativistic effects of the electron wave functions. This estimation is carefully done in [13], and the atomic EDM  $d_Z^{\text{atom}}$  can be written as

$$d_Z^{\text{atom}} \simeq C_1 (Z\alpha)^2 (1 + 2(Z\alpha)^2) d_e. \quad (4.1)$$

If we take  $C_1 \sim -100$ , then we obtain for Nitrogen and Tl cases,

$$d_N \simeq -0.3d_e \quad (4.2a)$$

$$d_{Tl} \simeq -60d_e \quad (4.2b)$$

where the sign in front of the number is not determined from eq.(4.1) since it depends on each atomic state.

The elaborate calculation for  $T\ell$  case shows

$$d_{T\ell} \simeq -585d_e. \quad (4.2c)$$

The order of magnitude enhancement may come from the atomic state configuration.

### B. Proton EDM in atomic system

As we discussed in section 2, the proton EDM mainly comes from the nuclear excitations. The proton EDM contribution to the atomic EDM can be written as

$$d_Z \simeq 0.03Zd_p. \quad (4.3)$$

In this case, we obtain for Nitrogen and  $T\ell$  cases,

$$d_N \simeq -0.2d_p \quad (4.4a)$$

$$d_{T\ell} \simeq 2.4d_p. \quad (4.4b)$$

On the other hand, as we saw in section 2, the elaborate calculations show

$$d_N \simeq -0.16d_p \quad (4.4c)$$

$$d_{T\ell} \simeq 4.8d_p. \quad (4.4d)$$

As can be seen from eqs.(4.4), the qualitative formula of eq.(4.3) gives sufficiently reliable estimations of the nuclear EDM.

### C. $d_e$ and $d_p$ from SUSY models

Now, as we saw in the previous section, the relation between the  $d_e$  and  $d_p$  EDMs from the SUSY model calculations are shown in fig. 1. If we choose the values of  $M_2$  and  $m_0$  to be

$$M_2 \simeq 9 \text{ TeV}, \quad m_0 \simeq 9 \text{ TeV}$$

then we obtain

$$d_e \simeq -2.8 \times 10^{-31} \text{ e} \cdot \text{cm} \quad (4.5a)$$

$$d_p \simeq -1.9 \times 10^{-29} \text{ e} \cdot \text{cm}. \quad (4.5b)$$

In this case, the atomic EDM for Nitrogen and  $T\ell$  cases from the electron EDM become

$$d_N^e \simeq -1.0 \times 10^{-31} \text{ e} \cdot \text{cm} \quad (4.6a)$$

$$d_{T\ell}^e \simeq -(0.2 \sim 1.8) \times 10^{-28} \text{ e} \cdot \text{cm}. \quad (4.6b)$$

On the other hand, we obtain the atomic EDM for Nitrogen and  $T\ell$  cases from the proton EDM contribution as

$$d_N^p \simeq -0.4 \times 10^{-29} \text{ e} \cdot \text{cm}. \quad (4.6c)$$

$$d_{T\ell}^p \simeq -1.0 \times 10^{-28} \text{ e} \cdot \text{cm}. \quad (4.6d)$$

Therefore, the EDM contributions from the electron (relativistic effects) and the proton (nuclear finite size effects) for the  $T\ell$  case may well be comparable. But the atomic EDM for the Nitrogen case is mainly determined from the proton EDM.

## V. CONCLUSIONS

We have presented the proton and neutron EDMs which are extracted from the atomic EDM measurements. In particular, we show that the proton EDM can be obtained if one can measure the EDM of Nitrogen atomic systems. The EDM measurement of Nitrogen atomic system enables to discuss the flavor dependence of the quark EDM which should give some important information on the origin of the T-violation in field theory models.

Also, we have studied the EDM of neutron, proton and electron in the minimal supersymmetric standard model. In the presence of supersymmetric CP-violation, the new limit on the neutron EDM extracted from atomic systems excludes a wide parameter region of SUSY breaking masses above 1 TeV, while the old limit excludes only a small mass region below 1 TeV. Thus the observed neutron EDM is found to give a very stringent test on the supersymmetric model.

---

[1] K. Abe et al. [Belle collaboration], Phys. Rev. **D67**,031102 (2003)

[2] B. Aubert et al. [BaBar collaboration], hep-th/0207070

- [3] P.G. Harris et al., Phys. Rev. Lett. **82**, 904 (1999)
- [4] I.S. Altarev et al., Phys. Atom. Nucl. **59**, 1152 (1996)
- [5] K.F.Smith et al., Phys. Lett. **B234**, 191 (1990)
- [6] M.A.Rosenberry and T.E. Chupp, Phys. Rev. Lett. **86**, 22 (2001)
- [7] T.G. Vold, F.G. Raab, B. Heckel, and N. Fortson, Phys. Rev. Lett. **52**, 2229 (1984)
- [8] M.V. Romalis, W.C. Griffith, J.P. Jacobs, and N. Fortson, Phys. Rev. Lett. **86**, 2505 (2001)
- [9] S.K.Lamoreaux, J.P. Jacobs, B. Heckel, F.G. Raab, and N. Fortson, Phys. Rev. Lett. **59**, 2275 (1987)
- [10] L.I.Schiff, Phys. Rev. **132**, 2194 (1963)
- [11] P.G.H.Sandars, Phys. Lett. **14**, 194 (1965)
- [12] P.G.H.Sandars, Phys. Lett. **22**, 290 (1966); J. Phys.**B1**, 511 (1968)
- [13] T. Asaga, T. Fujita and M. Hiramoto, Prog. Theor. Phys. **106**, 1223 (2001)
- [14] I.B.Khriplovich, S.K.Lamoreaux, *CP Violation Without Strangeness*, Springer 1997
- [15] S. Oshima, T. Fujita and T. Asaga, nucl-th/0412071
- [16] For reviews on supersymmetric models, see for instance, H.P. Nilles, Phys. Rep. **110**, 1 (1984).
- [17] T. Goto, Y.Y. Keum, T. Nihei, Y. Okada and Y. Shimizu, Phys. Lett. **B460**, 333 (1999).
- [18] B.C. Regan, E.D. Commins, C.J. Schmidt and D. DeMille, Phys. Rev. Lett. **88**, 071805-1 (2002)
- [19] D. Cho, K. Sangster, and E.A. Hinds Phys. Rev. **A44**, 2783 (1991)
- [20] Z.W. Liu and H.P. Kelly, Phys. Rev. **A45**, R4210 (1992)
- [21] Y. Kizukuri and N. Oshimo, Phys. Rev. **D46**, 3025 (1992)
- [22] A.G. Cohen, D.B. Kaplan, and A.E. Nelson, Phys. Lett. **B388**, 588 (1996)
- [23] T. Ibrahim and P. Nath, Phys. Rev. **D57**, 478 (1998).
- [24] I.B. Khriplovich and K.N. Zyablyuk, Phys. Lett. **B383**, 429 (1996); T. Falk, K.A. Olive, M. Pospelov and R. Roiban, Nucl. Phys. **B560**, 3 (1999); J. Hisano and Y. Shimizu, Phys. Lett. **B581**, 224 (2004).

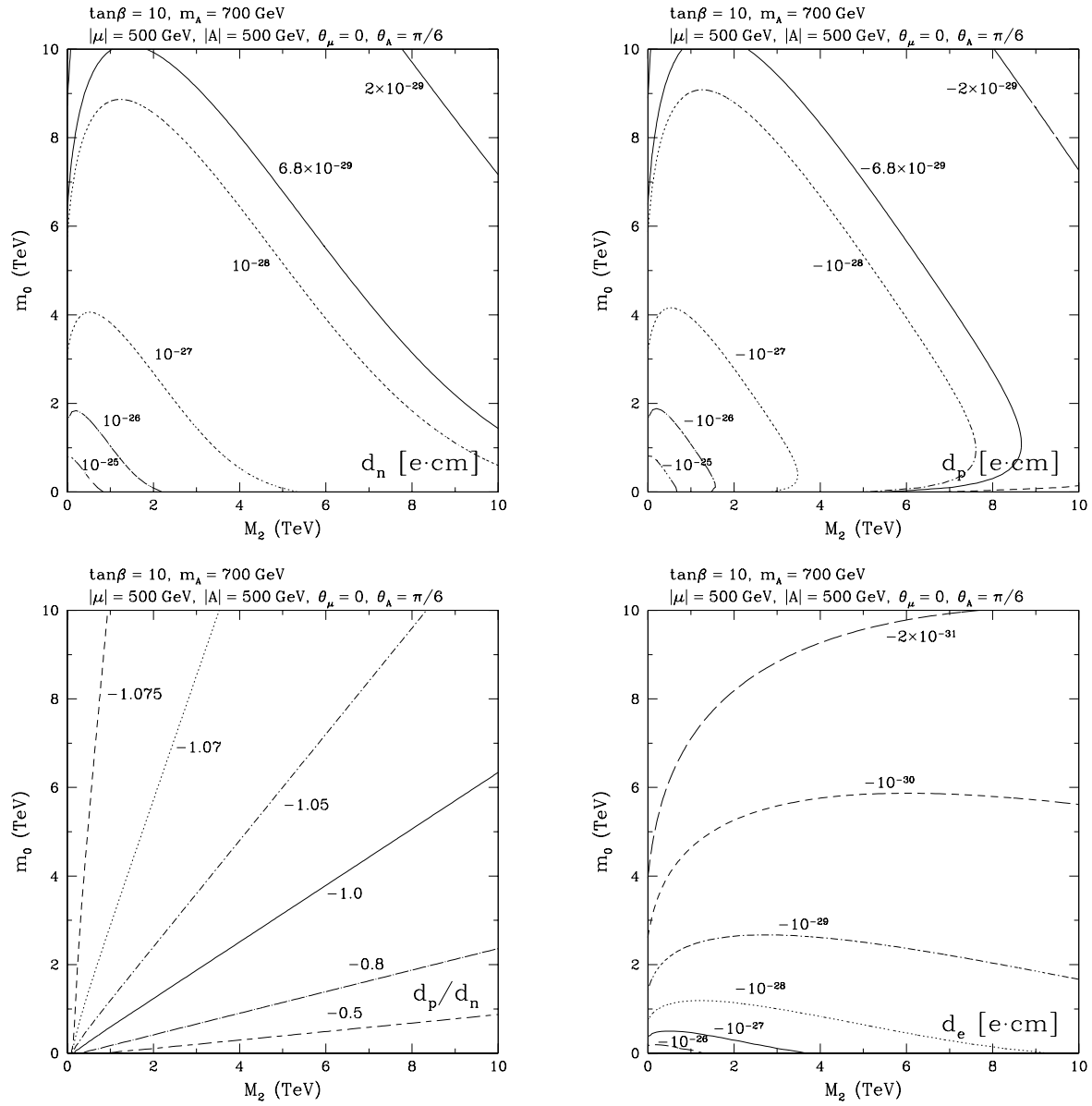


FIG. 1: Contour plots of  $d_n$  (upper left window),  $d_p$  (upper right window),  $d_p/d_n$  (lower left window) and  $d_e$  (lower right window) in the  $(M_2, m_0)$  plane for  $\tan\beta = 10$ ,  $m_A = 700$  GeV,  $|\mu| = 500$  GeV,  $|A| = 500$  GeV,  $\theta_\mu = 0$ ,  $\theta_A = \pi/6$ .



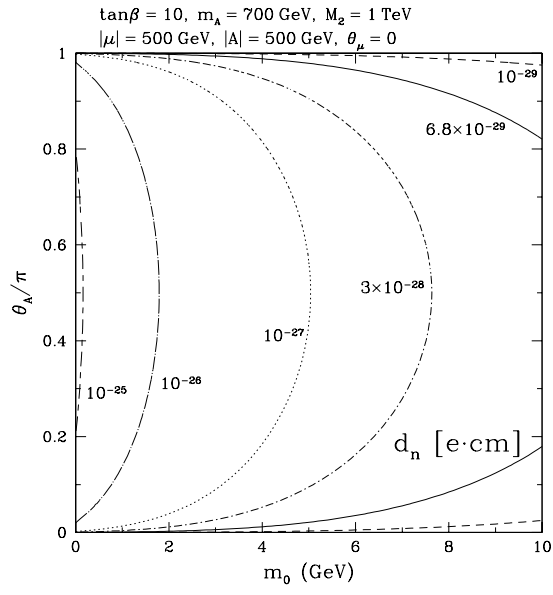


FIG. 2: Contours of  $d_n$  in the  $(m_0, \theta_A)$  plane for  $\tan\beta = 10$ ,  $m_A = 700$  GeV,  $M_2 = 1$  TeV,  $|\mu| = 500$  GeV,  $|A| = 500$  GeV,  $\theta_\mu = 0$ .

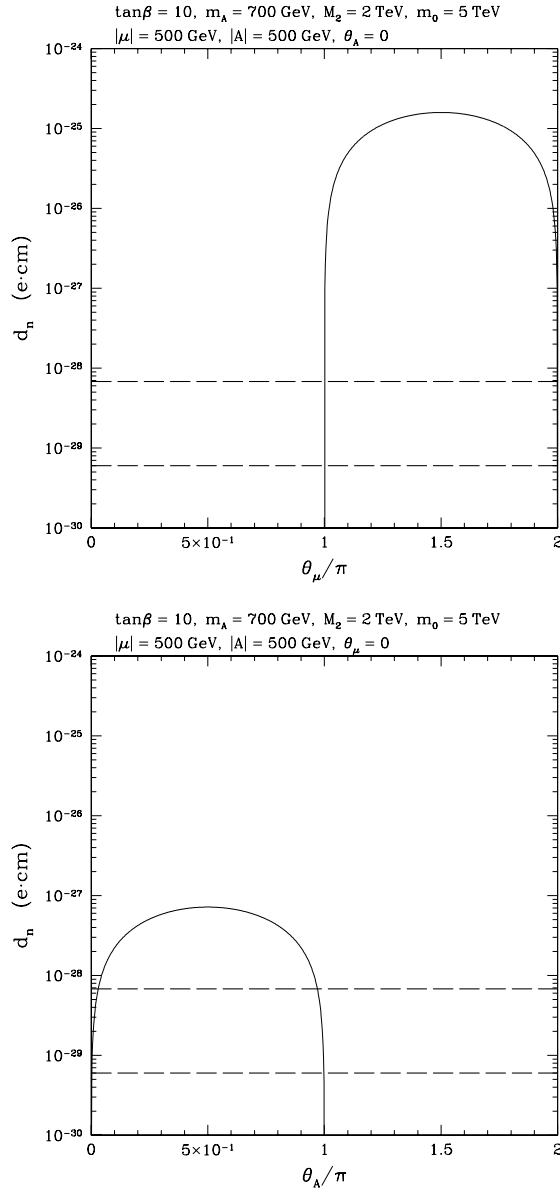


FIG. 3: The neutron EDM  $d_n$  vs  $\theta_\mu$  (upper window) and  $\theta_A$  (lower window). Relevant supersymmetric parameters for the upper window are chosen as  $\tan\beta = 10$ ,  $m_A = 700 \text{ GeV}$ ,  $M_2 = 2 \text{ TeV}$ ,  $m_0 = 5 \text{ TeV}$ ,  $|\mu| = 500 \text{ GeV}$ ,  $|A| = 500 \text{ GeV}$  and  $\theta_A = 0$ , while those for the lower window are the same except  $\theta_\mu = 0$ . The range  $0 < \theta_\mu < \pi$  in the upper window and  $\pi < \theta_A < 2\pi$  in the lower window corresponds to  $d_n < 0$ . In the region between the two dashed lines, the EDM constraint  $0.06 \times 10^{-28} \text{ e}\cdot\text{cm} < d_n < 0.68 \times 10^{-28} \text{ e}\cdot\text{cm}$  is satisfied.